Biology Contribution

Expression of EGFR Under Tumor Hypoxia: Identification of a Subpopulation of Tumor Cells Responsible for Aggressiveness and Treatment Resistance

Ilse J. Hoogsteen, M.D., Ph.D.,* Henri A.M. Marres, M.D., Ph.D.,[†]
Franciscus J.A. van den Hoogen, M.D., Ph.D.,[†] Paul F.J.W. Rijken, MSc.,*
Jasper Lok, BSc.,* Johan Bussink, M.D., Ph.D.,* and
Johannes H.A.M. Kaanders, M.D., Ph.D.*

*Departments of *Radiation Oncology and [†]Otorhinolaryngology/Head-Neck Surgery, Radboud University Nijmegen Medical Centre, Nijmegen, The Netherlands*

Summary

Hypoxia and overexpression of EGFR are common characteristics of head-and-neck cancers. Colocalization of both factors might define a critical subpopulation responsible for local recurrence, metastasis formation, or treatment resistance. In the present study colocalization with hypoxia was found in a series of head-and-neck squamous cell carcinomas. The amount of colocalization was associated with outcome, indicating a survival advantage for hypoxic cells expressing EGFR.

Purpose: Overexpression of epidermal growth factor receptor (EGFR) and tumor hypoxia have been shown to correlate with worse outcome in several types of cancer including head-and-neck squamous cell carcinoma. Little is known about the combination and possible interactions between the two phenomena.

Methods and Materials: In this study, 45 cases of histologically confirmed squamous cell carcinomas of the head and neck were analyzed. All patients received intravenous infusions of the exogenous hypoxia marker pimonidazole prior to biopsy. Presence of EGFR, pimonidazole binding, and colocalization between EGFR and tumor hypoxia were examined using immunohistochemistry.

Results: Of all biopsies examined, respectively, 91% and 60% demonstrated EGFR- and pimonidazole-positive areas. A weak but significant association was found between the hypoxic fractions of pimonidazole (HFpimo) and EGFR fractions (F-EGFR) and between F-EGFR and relative vascular area. Various degrees of colocalization between hypoxia and EGFR were found, increasing with distance from the vasculature. A high fraction of EGFR was correlated with better disease-free and metastasis-free survival, whereas a high degree of colocalization correlated with poor outcome.

Conclusions: Colocalization of hypoxia and EGFR was demonstrated in head-and-neck squamous cell carcinomas, predominantly at longer distances from vessels. A large amount of colocalization was associated with poor outcome, which points to a survival advantage of hypoxic cells that are also able to express EGFR. This subpopulation of tumor cells might be indicative of tumor aggressiveness and be partly responsible for treatment resistance.

Reprint requests to: Ilse J. Hoogsteen, M.D., Ph.D., Department of Radiation Oncology, 874, Radboud University Nijmegen Medical Centre, PO Box 9101, 6500 HB Nijmegen, The Netherlands. Tel: 31-24-3614515; Fax: 31-24-3610792; E-mail: i.hoogsteen@rther.umcn.nl

Introduction

Squamous cell carcinoma of the head and neck (HNSCC) is a significant cause of morbidity and mortality, with approximately 600,000 new cases worldwide (1). Much effort has been put into developing novel agents and optimizing treatment focusing on organ preservation and improvement of survival (2). Information on the molecular status of head-and-neck cancer and the ability to develop specific molecular profiles would permit optimization and selection of the appropriate therapy for the individual patient with less toxicity.

One key factor that plays a central role in HNSCC is the epidermal growth factor receptor (EGFR). EGFR belongs to the ErbB/HER family of tyrosine kinases. It is a membrane-associated receptor, and ligand binding induces activation of the intrinsic kinase domain, leading to stimulation of various downstream signaling pathways (3). Triggering this network mediates a multitude of cellular responses including cell growth, proliferation, apoptosis, migration, and angiogenesis (4). Overexpression of EGFR was found in most epithelial malignancies including HNSCC, and it has been shown to correlate with worse outcome in HNSCC (3, 5).

Another important aspect of solid tumors is tumor hypoxia. It has a strong effect on tumor cell biology, providing an overall selective advantage for malignant growth. It promotes genetic and proteomic changes leading to increased metastasis, angiogenesis, and selection of cells with diminished apoptotic potential (6). Tumor hypoxia has been associated with worse outcome in various types of cancer, including HNSCC (7).

Inhibitors of EGFR are among the most promising molecular targeting agents for combination with radiotherapy (2), and the same accounts for therapies directed at counteracting tumor hypoxia (8). Despite the importance of EGFR and tumor hypoxia in cancer development, both strategies have had limited success thus far. Detailed understanding of the underlying mechanisms is therefore necessary. Colocalization of both factors might define a critical subpopulation responsible for local recurrence, metastasis formation, or treatment resistance. The purpose of the present study was to investigate the presence of EGFR and colocalization with hypoxia in HNSCC.

Methods and Materials

Patients

Between 1998 and 2002, 53 patients with HNSCC were included in our hypoxia marker study at the Radboud University Nijmegen Medical Centre. Patients with primary stage II-IV squamous cell carcinoma of the oral cavity, oropharynx, hypopharynx, or larynx were enrolled. Approval from the local ethics committee was obtained.

Approximately 2 h before patients underwent biopsies, they received a 20-min intravenous infusion of the hypoxia marker pimonidazole hydrochloride (500 mg/m^2; Hypoxyprobe-1; NPI, Inc., Belmont, MA). Biopsy samples were taken for routine diagnostic purposes, and additional biopsy samples were taken for hypoxia marker analysis. The latter samples were snap frozen in liquid nitrogen until immunohistochemical processing.

Immunohistochemical staining

From frozen biopsy material, sections of 5 μm were cut and mounted on poly-L-lysine coated slides, followed by fixation in acetone at 4°C and rehydration in phosphate-buffered saline (PBS; Klinipath, Duiven, The Netherlands). Sections were incubated in primary antibody diluent (PAD; GeneTex Inc., San Antonio, TX) for 5 min at room temperature. Sections were incubated overnight at 4°C with goat-anti-EGFR antibody (Santa Cruz Biotechnology, Santa Cruz, CA) diluted 1:50 in PAD, followed by incubation with donkey-anti-goat Cy3 antibody (Jackson Immunoresearch Laboratories, West Grove, PA) at 1:600 dilution in PBS. For detection of pimonidazole, sections were incubated with rabbit-anti-pimo antibody (from J.A. Raleigh, Department of Radiation Oncology and Toxicology, University of North Carolina, Chapel Hill) diluted 1:1,000 in PAD, followed by incubation with donkey-anti-rabbit Alexa488 (Molecular Probes, Leiden, The Netherlands) antibody diluted 1:600 in PBS. Sections were rinsed with PBS and stained for vessels by incubation with mouse antibody PAL-E (Euro Diagnostica, Arnhem, The Netherlands) diluted 1:10 in PAD, followed by incubation with chicken-anti-mouse Alexa647 antibody (Molecular Probes) 1:100 in PBS. Sections were mounted in Fluorostab (ProGen Biotechnik GmbH, Heidelberg, Germany).

Image acquisition

Tissue sections were scanned using a digital image processing system consisting of a high-resolution 12-byte charge-coupled device camera (Micromax; Roper Scientific, Trenton, NJ) on a fluorescence microscope (Axioskop, Zeiss, Göttingen, Germany) and a computer-controlled motorized stepping stage. Image processing was done using IPLab software (Scanalytics, Inc., Fairfax, VA) on a Macintosh (Cupertino, CA) computer. Each tissue section was scanned for pimonidazole, EGFR, and vessel signals at ×200 magnification. Resulting composite gray-scale images were converted to binary images for further analysis. Thresholds for segmentation of the fluorescent signals were interactively set at intensities where the steepest gradient occurred between background and foreground intensity levels. Different intensities of EGFR expression were observed. To investigate a potential influence, the intensity of EGFR staining was also interpreted semiquantitatively by visual inspection at ×100 magnification. Biopsy results were divided into three groups according to weak, moderate, and strong intensity levels. To facilitate further analysis, in these particular groups, thresholds for segmentation were set at the same levels. The corresponding composite binary images were superimposed onto one pseudo-colored image for visual evaluation.

Analysis

For examination of immunohistochemical staining, one complete section per tumor was investigated. Tumor area delineation was guided by hematoxylin-eosin staining. This delineated area was subsequently used as a mask in further analysis from which nontumor tissue, necrotic areas, and artifacts were excluded. The fractions based on pimonidazole (hypoxic fraction; HFpimo) and EGFR staining (F-EGFR) were defined as the tumor area positive for pimonidazole or EGFR, relative to the total tumor area. Vascular density was calculated as the number of vascular

structures per square millimeter, and the relative vascular area (RVA) was defined as the PAL-E positive area divided by the total tumor area (pixels). To determine colocalization of EGFR and pimonidazole, the fraction of the total EGFR-stained area that was also positive for pimonidazole was measured. The area positive for both pimonidazole and EGFR was divided by the total EGFR-positive area (F-EGFR$_{[pimo]}$). To determine the distribution of hypoxia, EGFR, and colocalization of both parameters in relation to the vasculature, zones were chosen arbitrarily at increasing distances from the surface of the nearest vessel (<50 μm, 50−100 μm, 101−150 μm, 151−200 μm, 201−250 μm, and >250 μm), and for each parameter, a zonal fraction was calculated.

Statistical methods

Statistical analyses were carried out with a Macintosh computer using Prism version 4.0 software (Hearne Scientific Software, Dublin, Ireland). Correlations between the different parameters were assessed using the Pearson chi-squared test. To determine correlations and differences between these parameters and categorical tumor characteristics the Spearman correlation coefficient and one-way analysis of variance tests were applied. Survival rates were calculated from the date of histological diagnosis using the Kaplan-Meier method, and the log−rank test was used to test for differences between survival rates. A p value of ≤0.05 was considered statistically significant.

Results

Patients and treatment

This study included 53 patients. Pimonidazole was given to all patients before biopsies were performed, and none of the patients had adverse reactions. Three patients were excluded from the final analysis because the biopsy result was of poor quality, attributable to mechanical damage during staining or biopsy. It was observed that in five biopsies, EGFR was found in the nuclei of cells only. Because of the unclear role of nuclear EGFR in HNSCC, these biopsies were considered a separate group and were not included in further analysis of the membranous EGFR, but they were analyzed separately. Thus, 45 histologically confirmed cases of HNSCC were analyzed. Table 1 shows patient and tumor characteristics.

Pimonidazole, EGFR, and vessel staining

All markers gave strong and bright fluorescent signals with little background, except in areas of necrosis and occasionally in stromal components of the tumor. Pimonidazole binding was observed in the cytoplasm, whereas EGFR staining was predominantly confined to the cell membrane. Besides membrane staining, in approximately 25% of biopsies, EGFR was also observed in the nucleus of the cell. The membranous expression pattern, however, was strongly dominant. Nuclear EGFR could be seen in both well-oxygenated and hypoxic regions. In five biopsies, EGFR was confined to nuclei. Interestingly, in some of these biopsies, no or very little pimonidazole binding could be detected, indicating that these tumors are well oxygenated.

Different intensities of EGFR staining could be observed, and biopsy sample intensities were therefore divided into three groups,

namely, weak ($n = 27$), moderate ($n = 13$), and strong ($n = 5$). Figure 1 shows examples of EGFR expression with different intensity levels and hypoxia represented by pimonidazole binding. Pimonidazole binding usually increased farther away from the blood vessels and could frequently be observed near necrosis. EGFR was more diffuse in the tumor, with the highest expression levels at intermediate distances (50−100 μm and 101−150 μm) from the blood vessels. Mean, median, and range values for all parameters are shown in Table 2.

Of all biopsy results, 91% and 60% demonstrated EGFR and pimonidazole positive areas (≥1% of the tumor area), respectively. A weak but significant correlation between F-EGFR and HFpimo could be found ($r = 0.35$, $p = 0.018$) (Fig 2A). Also, a weak association was found between F-EGFR and RVA ($r = 0.38$, $p = 0.005$) (Fig 2B). No other significant correlations could be demonstrated between parameters. Between the micro-environmental parameters tested and known tumor characteristics such as T stage, N stage, tumor site and differentiation grade, no correlations were observed.

Colocalization between pimonidazole and EGFR

Among biopsy samples, various degrees of colocalization between pimonidazole and EGFR could be found, with a maximum of

Table 1 Patient and tumor characteristics

Characteristic	No. of patients
Gender	
Man	39
Woman	6
Tumor site	
Larynx	21
Hypopharynx	11
Oropharynx	11
Oral cavity	2
T stage*	
T1	3
T2	13
T3	19
T4	10
N stage	
N0	13
N1	13
N2	18
N3	1
Histopathological grade	
Good	2
Moderate	23
Poor	18
Not classified	2
Treatment	
Primary radiotherapy	30
Conventional fractionation	5
Accelerated	24
Palliative schedule	1
Concurrent chemoradiotherapy	5
Surgery and adjuvant radiotherapy	7
No treatment	3[†]

* All patients were stage M0.
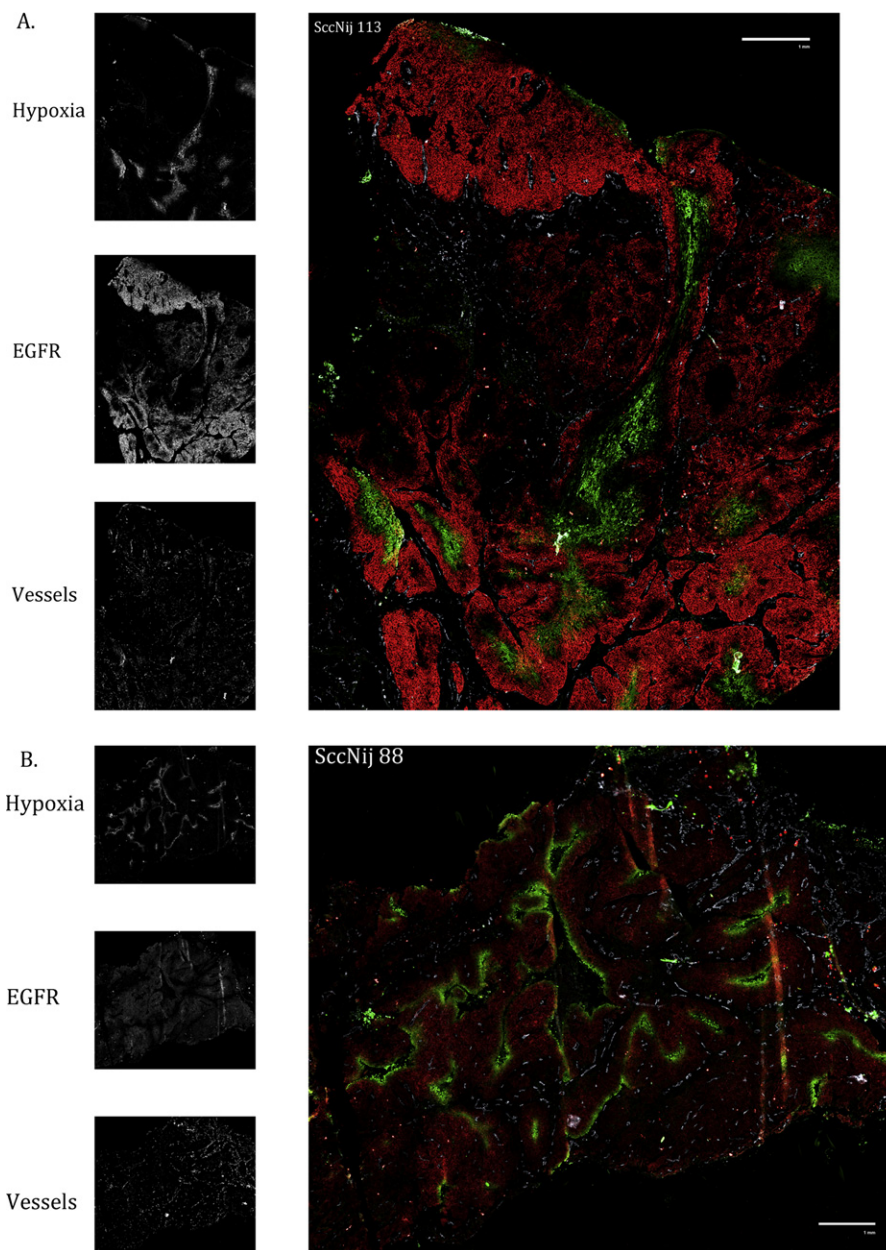[†] All patients died before treatment could start.

Fig. 1. Merged fluorescent colored images of biopsy samples from two oropharyngeal carcinomas, both showing tumor hypoxia (pimonidazole binding, green), EGFR expression (red), and vessels (white). (A) High EGFR intensity and (B) low EGFR intensity. Original single channel images (gray value) for each parameter are also shown.

24%. In a single biopsy sample, areas of colocalization could be found but also areas of mismatch. In some samples with pimonidazole binding and EGFR expression, no colocalization could be detected, and EGFR was then present mainly in better oxygenated areas. When colocalization was observed, it usually increased with distance from the blood vessels (with largest amount at $\geq$250 μm). Figure 3 shows an example of EGFR expression in a hypoxic area.

Survival analysis

For survival analysis, the patient group was divided by the median values for HFpimo, F-EGFR, and F-EGFR$_{[pimo]}$

(Fig. 4). For HFpimo, no significant differences between the subgroups were observed for the various endpoints. For F-EGFR, no difference between the subgroups was found in locoregional control rate; however, a weak significant difference ($p = 0.05$) was found in metastasis-free survival, and a 5-year disease-free survival rate of 60% vs. 31%, respectively, for patients with a high F-EGFR and patients with a low F-EGFR ($p = 0.02$) could be demonstrated. This was also repeated for the different treatment groups, and it was found consistently that patients with a high F-EGFR treated with accelerated radiotherapy alone had better survival (data not shown). The 5 patients from whom biopsy samples demonstrated only nuclear EGFR had a comparable 5-year locoregional control rate (75%) and a slightly better 5-year disease-free survival rate (41%) than

Table 2   Values for hypoxic and vascular parameters in 45 biopsies of head and neck squamous cell carcinomas

Parameter	HFpimo (%)	F-EGFR (%)	VD (N/mm^2)	RVA (%)	F-EGFR$_{[pimo]}$ (%)
Mean	3.4	16.1	341.6	1.0	4.6
Median	1.2	9.6	292.6	0.7	2.7
Range	0−14.1	0−61.5	153.6−853.2	0.2−3.4	0−24.3
SD	3.9	15.8	158.5	0.7	5.6

Abbreviations: F-EGFR = EGFR fraction; F-EGFR$_{[pimo]}$ = area positive for both pimonidazole and EGFR divided by the total EGFR-positive area; HFpimo = pimonidazole hypoxic fraction; RVA = relative vascular area; SD = standard deviation; VD = vascular density.

the patients with a low F-EGFR. No significant differences were found.

For F-EGFR$_{[pimo]}$, a significant difference was found between the locoregional control rates of the groups ($p = 0.03$). Five-year locoregional control was 77% for patients with low F-EGFR$_{[pimo]}$ vs. 38% for patients with high values. A high F-EGFR$_{[pimo]}$ showed a trend toward worse disease-free survival ($p = 0.06$). No significant difference was observed in metastasis-free survival. Chi-square test results did not indicate any significant differences in distribution of T stage, tumor site, and treatment modality between the two subgroups. Stratification into three groups for staining intensity of EGFR yielded no significant differences for locoregional control or metastasis-free and disease-free survival rates.

Discussion

The principle aim of the present study was to explore the presence of EGFR under hypoxic conditions. With the triple-staining method used in this study, colocalization of hypoxia and EGFR was found with increasing distance from blood vessels. This suggests that a subpopulation of tumor cells exists under hypoxic conditions expressing EGFR that might be relevant for clinical outcome. This hypothesis is supported by the results shown here, where the amount of colocalization between hypoxia and EGFR was significantly associated with worse locoregional control. Furthermore, a trend toward an association with disease-free

survival was observed. Although the sample size was small and interpretation of data should be done carefully, it points to a survival advantage of hypoxic cells that are also able to express EGFR. To our knowledge, this is the first clinical study exploring the relationship between EGFR and hypoxia in HNSCC and demonstrating such a relationship. The potential influence on outcome is currently being investigated further in a large randomized trial using oxygenation modification in laryngeal cancer (8, 9).

Intensive research has recently focused on EGFR as the potential target for cancer therapy. In the present study, 90% of the biopsy samples examined demonstrated weak to strong membranous expression of EGFR. This finding is in agreement with those of earlier studies in which at least 80% of all HNSCC EGFR was found to be overexpressed compared to the level in normal mucosa of patients without cancer (5, 10). In 25% of the samples, incidental nuclear EGFR staining was observed, and five samples demonstrated exclusively nuclear EGFR staining. The clinical significance of this phenomenon is unclear, and we are currently investigating this in a larger cohort of patients.

Another clinically relevant obstacle is tumor hypoxia. Hypoxia is considered one of the causes of radioresistance. Clinical studies in HNSCC (7) and uterine cervix (6) have demonstrated a significant correlation between hypoxia and poor response to radiotherapy. In this study, a positive, albeit weak, relationship between hypoxia and fraction EGFR was found. In studies from the 1980s, it was found that a reduction in oxygen probably inhibits EGFR down-regulation (11). Furthermore, exposure of different human
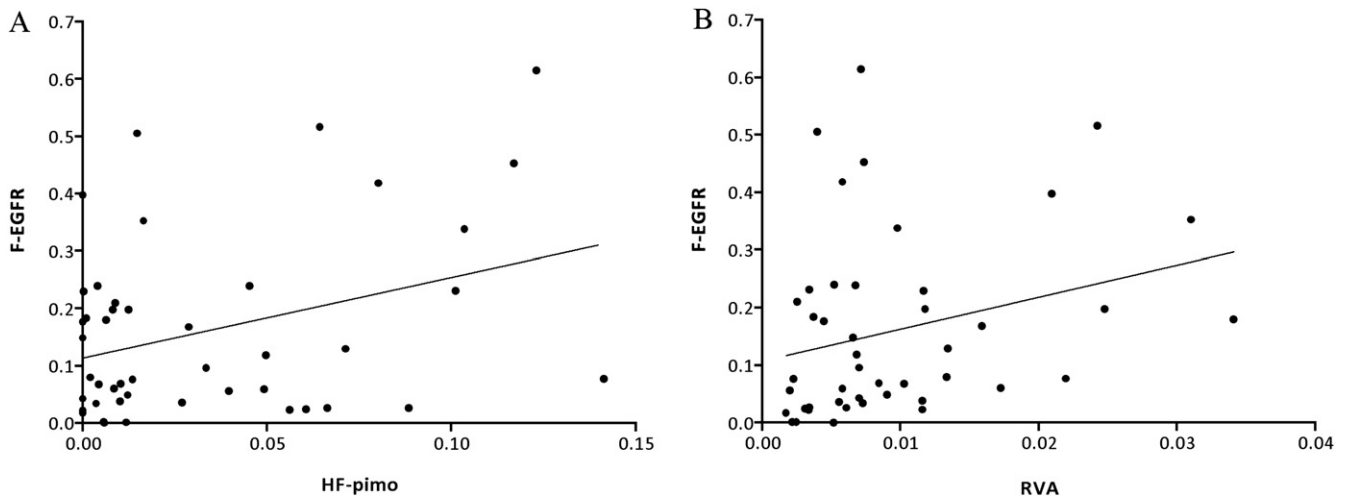

Fig. 2.   Scatterplots comparing F-EGFR with HFpimo (A) and F-EGFR with RVA (B) in 45 head-and-neck squamous cell carcinoma patients. Linear best fit is shown.
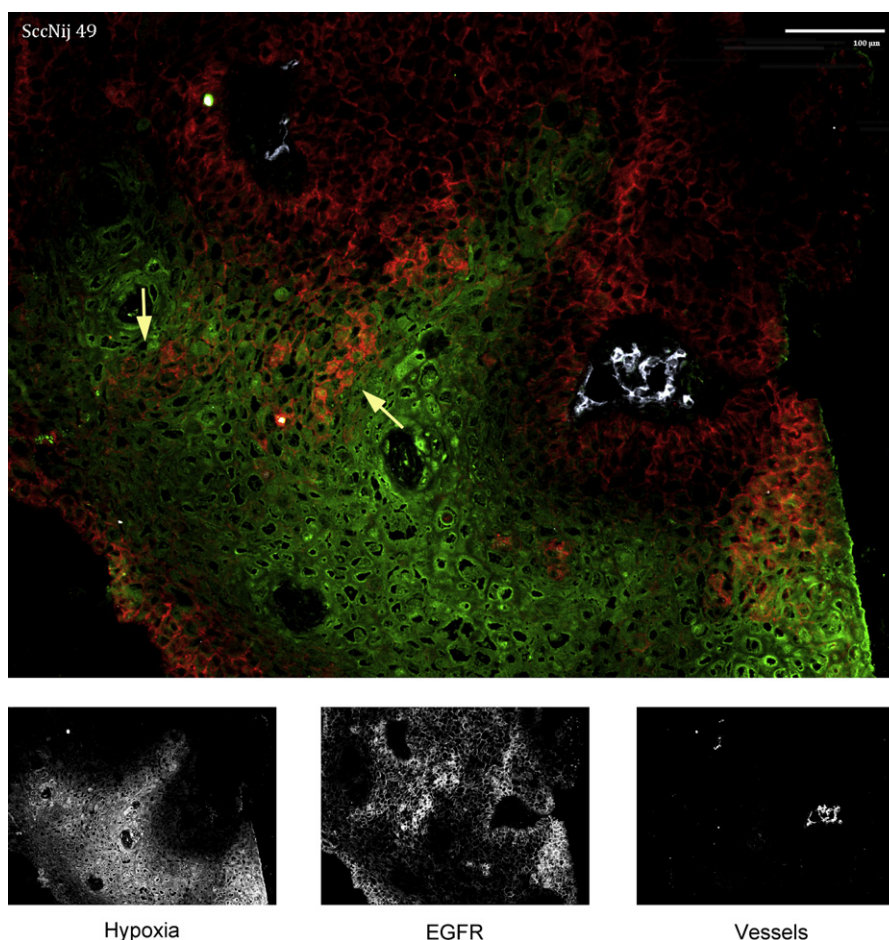
Fig. 3. Merged fluorescent image of a biopsy sample from a hypopharyngeal carcinoma SccNij49, showing EGFR expression (red) under hypoxia (green) (arrows). Colocalization was found at increasing distance from the blood vessels (white).

tumor cell lines to hypoxia induced EGFR expression compared to aerobic cells (12). From these studies, it can be concluded that most observations underscore a role for hypoxia in inducing expression of EGFR, which is in agreement with the results obtained here. Improved understanding of this process will provide a mechanistic basis for optimization of treatment strategies.

EGFR, in turn, also increases the response to hypoxia by inducing proteins that promote cellular survival. From previous studies in tumor cell lines, it is known that EGFR is involved in the response to hypoxia through one of its major downstream targets, the PI3-K/Akt pathway (13). Blockage of this pathway results in a dramatic reduction of hypoxic tumor cell viability and contributes to an improvement of tumor control (14). To some extent, several hypoxia-related markers such as hypoxia-inducible transcription factor 1 (HIF-1) and carbonic anhydrase IX (CA-IX) are under the control of the EGFR/P13-K/Akt pathway (4). Inhibition of EGFR resulted in not only downregulation of HIF-1α and CA-IX but also a decrease in hypoxia as measured with the nitroimidazole hypoxia-marker EF5 (15). This was explained by vascular normalization and improved blood flow. In the present study, a positive relationship between EGFR expression and RVA has been found. Although this seems to be in contradiction to the positive relationship between the fraction EGFR and the hypoxic fraction, the RVA does not take into account whether blood vessels are perfused or not, because of the absence of a good perfusion marker for human use, and the RVA only reflects the area

containing vascular structures. Activation of vascular endothelial growth factor (VEGF) through EGFR leads to the induction of neoangiogenesis, which is often disorganized and functionally impaired. These defects in turn contribute to tumor hypoxia. Blockade of VEGF by EGFR inhibition was shown to decrease angiogenesis, leading to normalization of vasculature, an increase in blood perfusion, and a reduction in hypoxia (16). These results implicate an important role for EGFR in hypoxic tumor cells by promoting cellular survival and providing a powerful adaptive advantage during carcinogenesis.

Surprisingly, it was found that for patients with a high fraction of EGFR, time to disease recurrence was significantly longer. The presence of EGFR has been related to poor locoregional control in head-and-neck carcinomas treated with conventional radiotherapy by Ang *et al*. (5). Only patients who were randomized to the conventional radiotherapy arm of Radiation Therapy Oncology Group (RTOG) Phase III trial were included. Studies by Eriksen *et al*. (10) and Bentzen *et al*. (17) demonstrated that tumors with high EGFR expression levels benefit most from, respectively, accelerated radiotherapy and continuous hyperfractionated accelerated radiotherapy with an increase in locoregional control and disease-specific survival, while there was no benefit of acceleration for tumors with low EGFR. Increased activity of EGFR contributes to enhanced cellular proliferation and additionally an increase in their capacity for DNA damage repair, which may confer resistance to radiotherapy (18). This can be counteracted by
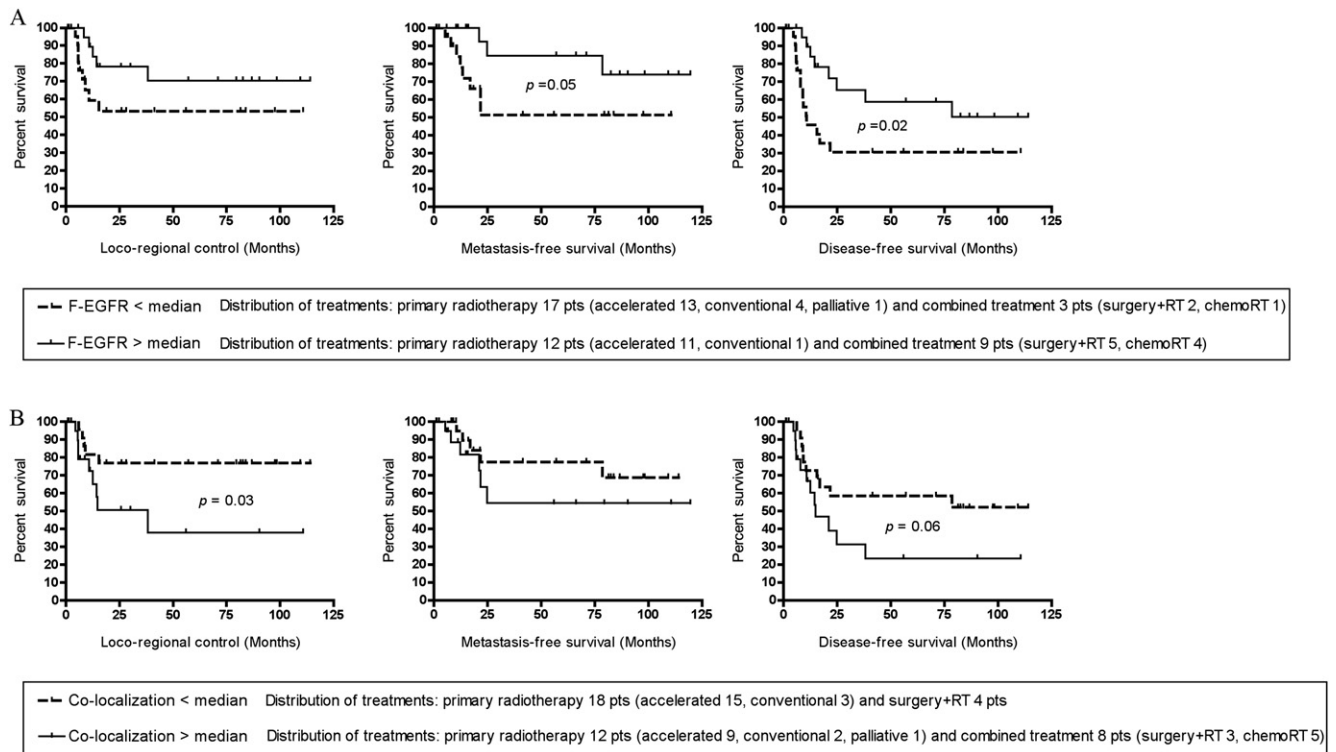
Fig. 4. Kaplan-Meier estimates for locoregional control and metastasis- and disease-free survival stratified by the median of F-EGFR (A) and F-EGFR$_{[pimo]}$ (B). Survival functions were compared using the log−rank test.

reducing overall treatment time with accelerated radiotherapy, explaining the preferential response to this approach in tumors with high EGFR expression (17). In this relatively small group of 45 patients, 25 patients underwent accelerated radiotherapy, and the same results were found for these patients, with a fraction of EGFR that was as high as that for the total group of patients. It is therefore possible that this may account for the positive correlation found between a high fraction EGFR and disease-free survival. Some remarks however, must be made regarding the present study. The population studied was rather small, and patients in this group underwent various treatments from surgery, conventional or accelerated radiotherapy with or without chemotherapy. Stratification by treatment modality left few cases per group for reliable statistical analyses.

Conclusions

In conclusion, it was possible to quantify colocalization of hypoxia assessed by the pimonidazole-binding assay and EGFR, which was further associated with poor locoregional control. This suggests not only a direct link between EGFR and hypoxia but also the fact that EGFR expression under hypoxic conditions may act as a survival factor for hypoxic tumor cells. This subpopulation of tumor cells might therefore be responsible for enhanced treatment resistance and ultimately poor outcome. Currently, all microenvironmental parameters are under investigation in a large series of laryngeal carcinomas included in our Phase III ARCON trial combining Accelerated Radiotherapy with CarbOgen breathing and Nicotinamide (9).

References

1. Marur S, Forastiere AA. Head and neck cancer: Changing epidemiology, diagnosis, and treatment. *Mayo Clin Proc* 2008;83:489−501.
2. Bonner JA, Harari PM, Giralt J, et al. Radiotherapy plus cetuximab for squamous cell carcinoma of the head and neck. *N Engl J Med* 2006; 354:567−578.
3. Hynes NE, Lane HA. ERBB receptors and cancer: The complexity of targeted inhibitors. *Nat Rev Cancer* 2005;5:341−354.
4. Yarden Y, Sliwkowski MX. Untangling the ErbB signaling network. *Nat Rev Mol Cell Biol* 2001;2:127−137.
5. Ang KK, Berkey BA, Tu X, et al. Impact of epidermal growth factor receptor expression on survival and pattern of relapse in patients with advanced head and neck carcinoma. *Cancer Res* 2002;62:7350−7356.
6. Vaupel P, Mayer A. Hypoxia in cancer: Significance and impact on clinical outcome. *Cancer Metastasis Rev* 2007;26(2):225−239.
7. Kaanders JHAM, Wijffels KIEM, Marres HAM, et al. Pimonidazole binding and tumor vascularity predict for treatment outcome in head and neck cancer. *Cancer Res* 2002;62:7066−7074.
8. Kaanders JHAM, Bussink J, van der Kogel AJ. Clinical studies of hypoxia modification in radiotherapy. *Semin Radiat Oncol* 2004;14: 233−240.
9. Kaanders JHAM, Bussink J, van der Kogel AJ. ARCON: A novel biology-based approach in radiotherapy. *Lancet Oncol* 2002;3: 728−737.
10. Bentzen SM, Atasoy BM, Daley FM, et al. Epidermal growth factor receptor expression in pretreatment biopsies from head and neck squamous cell carcinoma as a predictive factor for a benefit from accelerated therapy in a randomized controlled trial. *J Clin Oncol* 2005;24:5560−5567.
11. Wing DA, Talley GD, Storch TG. Oxygen concentration regulates EGF-induced proliferation and EGF-receptor down regulation. *Biochem Biophys Res Commun* 1988;153:952−958.

12. Franovic A, Gunaratnam L, Smith K, et al. Translational up-regulation of the EGFR by tumor hypoxia provides a nonmutational explanation for its overexpression in human cancer. *Proc Natl Acad Sci U S A* 2007;104:13092–13097.

13. Zhong H, Chiles K, Feldser D, et al. Modulation of hypoxia-inducible factor 1alpha expression by the epidermal growth factor/phophatidy-linositol 3-kinase/PTEN/AKT/FRAP pathway in human prostate cancer cells: Implications for tumor angiogenesis and therapeutics. *Cancer Res* 2000;60:1541–1545.

14. Krause M, Ostermann G, Petersen C, et al. Decreased repopulation as well as increased reoxygenation contribute to the improvement in local control after targeting of the EGFR by C225 during fractionated irradiation. *Radiother Oncol* 2005;76:162–167.

15. Qayum N, Muschel RJ, Im JH, et al. Tumor vascular changes mediated by inhibition of oncogenic signaling. *Cancer Res* 2009;69:6347–6354.

16. Morelli MP, Cascone T, Troiani T, et al. Anti-tumor activity of the combination of cetuximab, an anti-EGFR blocking monoclonal antibody and ZD6474, an inhibitor of VEGFR and EGFR tyrosine kinases. *J Cell Physiol* 2006;208:344–353.

17. Eriksen JG, Steiniche T, Overgaard J, et al. The role of epidermal growth factor receptor and E-cadherin for the outcome of reduction in the overall treatment time of radiotherapy of supraglottic larynx squamous cell carcinoma. *Acta Oncol* 2005;44:50–58.

18. Schmidt-Ullrich RK, Contessa JN, Dent P, et al. Molecular mechanisms of radiation-induced accelerated repopulation. *Radiat Oncol Invest* 1999;7:321–330.